



Modeling and Simulation of a Differential Roll Projectile

by Mark F. Costello

ARL-CR-455

July 2000

Approved for public release; distribution is unlimited.

DTIC QUALITY INSPECTED 4

20000928 035

The findings in this report are not to be construed as an official Department of the Army position unless so designated by other authorized documents.

Citation of manufacturer's or trade names does not constitute an official endorsement or approval of the use thereof.

Destroy this report when it is no longer needed. Do not return it to the originator.

Abstract

This report develops the equations of motion for a differential roll projectile configuration with seven degrees of freedom. The dynamic equations are generated generically such that the forward and aft components are mass unbalanced. A hydrodynamic bearing exists between the forward and aft components, which couples the roll degree of freedom. A simulation investigation shows that bearing resistance and forward/aft body mass ratio are the dominant factors in determining the roll dynamics. For spin rates typical of fin-stabilized projectiles, the trajectory is essentially independent of both bearing resistance and mass ratio.

Table of Contents

	<u>Page</u>
List of Figures	v
1. Introduction	1
2. Differential Roll Projectile Dynamic Model	2
3. Simulation Example	5
4. Conclusions	17
5. References	19
Appendix A: Constraint Forces and Moments	21
Appendix B: Rotation Kinetic Equations	27
List of Symbols	33
Distribution List	35
Report Documentation Page	41

INTENTIONALLY LEFT BLANK.

List of Figures

<u>Figure</u>	<u>Page</u>
1. Differential Roll Projectile Schematic	1
2. Range.....	6
3. Cross Range.....	6
4. Euler Pitch Angle	7
5. Euler Yaw Angle.....	7
6. Forward Body Velocity	8
7. Side Body Velocity.....	8
8. Vertical Body Velocity.....	9
9. Pitch Rate	9
10. Yaw Rate	10
11. Aerodynamic Angle of Attack.....	10
12. Roll Angle (Mass Ratio = 1%, Damping Coefficient = 0.01–0.000001)	11
13. Roll Rate (Mass Ratio = 1%, Damping Coefficient = 0.01–0.000001)	11
14. Roll Angle (Mass Ratio = 50%, Damping Coefficient = 0.01–0.000001)	12
15. Roll Rate (Mass Ratio = 50%, Damping Coefficient = 0.01–0.000001)	13
16. Roll Rate (Mass Ratio = 50%, Damping Coefficient = 0.01–0.000001)	13
17. Cross Range (Mass Ratio = 50%, Damping Coefficient = 0.01–0.000001)	14
18. Angle of Attack (Mass Ratio = 50%, Damping Coefficient = 0.01–0.000001)	14
19. Cross Range (Damping Coefficient = 0.0005, Mass Ratio = 1%–50%)	15
20. Roll Angle (Damping Coefficient = 0.0005, Mass Ratio = 1%–50%)	16

<u>Figure</u>	<u>Page</u>
21. Side Velocity (Damping Coefficient = 0.0005, Mass Ratio = 1%–50%)	16
22. Roll Rate (Damping Coefficient = 0.0005, Mass Ratio = 1%–50%)	17
A-1. Forces and Moments on the Forward Body	23
A-2. Forces and Moments on the Aft Body.....	23

1. Introduction

Compared to conventional munitions, smart munitions involve more design requirements due to additional sensors and control mechanisms. These additional components must seek to minimize the weight and space impact on the overall projectile design so that desired target effects can still be achieved with the weapon. The inherent design conflict between standard projectile design considerations and new requirements imposed by sensors and control mechanisms has led designers to consider more complex geometric configurations. One such configuration is the differential roll projectile. This projectile configuration is comprised of forward and aft components. The forward and aft components are connected through a bearing, which allows the forward and aft portions of the projectile to spin at different rates. Figure 1 shows a schematic of the differential roll projectile configuration.

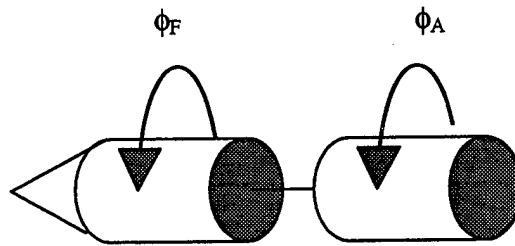


Figure 1. Differential Roll Projectile Schematic.

Typical flight mechanic analysis of a conventional, single-body, munition models the projectile with six degrees of freedom. Dynamic modeling of a differential roll projectile adds an additional roll degree of freedom to the equations of motion. This report begins with the development of a dynamic model of a differential roll projectile in atmospheric flight, including the additional roll degree of freedom. The model is derived such that both the forward and aft bodies can be mass unbalanced. A hydrodynamic bearing couples the forward and aft components in the roll axis. The mathematical model is utilized to show trends in system response as a function of mass ratio and bearing resistance.

2. Differential Roll Projectile Dynamic Model

The mathematical model describing the motion of the differential roll projectile allows for three translation and four rotation rigid-body degrees of freedom. The translation degrees of freedom are the three components of the mass center position vector. The rotation degrees of freedom are the Euler yaw and pitch angles, as well as the forward body roll and aft body roll angles. The equations presented here use the ground surface as an inertial reference frame [1].

Development of the kinematic and dynamic equations of motion is aided by the use of an intermediate reference frame. The sequence of rotations from the inertial frame to the forward and aft bodies consists of a set of body-fixed rotations that are ordered: yaw, pitch, and forward/aft body roll. The fixed-plane reference frame is defined as the intermediate frame before roll rotation. The fixed-plane frame is common to both the forward and aft bodies.

Equation (1) is the translation kinematic differential equations that relate time derivatives of the mass center position components to the mass center velocity components in fixed-plane reference frame.

$$\begin{Bmatrix} \dot{x} \\ \dot{y} \\ \dot{z} \end{Bmatrix} = \begin{bmatrix} c_\theta c_\psi & -s_\psi & s_\theta c_\psi \\ c_\theta s_\psi & c_\psi & s_\theta s_\psi \\ -s_\theta & 0 & c_\theta \end{bmatrix} \begin{Bmatrix} u \\ v \\ w \end{Bmatrix}. \quad (1)$$

Equation (2) is the rotation kinematic differential equations that relate time derivatives of the Euler angles with angular velocity components in the fixed-plane reference frame.

$$\begin{Bmatrix} \dot{\phi}_F \\ \dot{\phi}_A \\ \dot{\theta} \\ \dot{\psi} \end{Bmatrix} = \begin{bmatrix} 1 & 0 & 0 & t_\theta \\ 0 & 1 & 0 & t_\theta \\ 0 & 0 & 1 & 0 \\ 0 & 0 & 0 & 1/c_\theta \end{bmatrix} \begin{Bmatrix} p_F \\ p_A \\ q \\ r \end{Bmatrix}. \quad (2)$$

Equation (3) is the translation kinetic differential equations described in the fixed-plane reference frame.

$$\begin{Bmatrix} \dot{u} \\ \dot{v} \\ \dot{w} \end{Bmatrix} = \begin{Bmatrix} \frac{X}{m} \\ \frac{Y}{m} \\ \frac{Z}{m} \end{Bmatrix} - \begin{bmatrix} 0 & -r & q \\ r & 0 & 0 \\ -q & 0 & 0 \end{bmatrix} \begin{Bmatrix} u \\ v \\ w \end{Bmatrix}. \quad (3)$$

Equation (4) is the rotation kinetic differential equations described in the fixed-plane reference frame.

$$\begin{Bmatrix} \dot{p}_F \\ \dot{p}_A \\ \dot{q} \\ \dot{r} \end{Bmatrix} = [I]^{-1} \begin{Bmatrix} g_{F1} - M_V \\ g_{A1} + M_V \\ g_{F2} + g_{A2} \\ g_{F3} + g_{A3} \end{Bmatrix}. \quad (4)$$

A derivation of equation (4), along with definitions of the right side components, is provided in Appendices A and B.

As shown in equation (5), the total applied force on the complete configuration is provided by the weight of both the forward and aft bodies (w) and air loads (A).

$$\begin{Bmatrix} X \\ Y \\ Z \end{Bmatrix} = \begin{Bmatrix} X_w \\ Y_w \\ Z_w \end{Bmatrix} + \begin{Bmatrix} X_A \\ Y_A \\ Z_A \end{Bmatrix}. \quad (5)$$

The weight portion of the external loads is given by equation (6),

$$\begin{Bmatrix} X_w \\ Y_w \\ Z_w \end{Bmatrix} = mg \begin{Bmatrix} -s_\theta \\ 0 \\ c_\theta \end{Bmatrix}, \quad (6)$$

while the aerodynamic force contribution is given by equation (7),

$$\begin{Bmatrix} X_A \\ Y_A \\ Z_A \end{Bmatrix} = q_a D \begin{Bmatrix} C_{X0} + C_{XA2}\alpha^2 + C_{XB2}\beta^2 \\ C_{Y0} + C_{YB1}\beta \\ C_{Z0} + C_{ZA1}\alpha \end{Bmatrix}. \quad (7)$$

The longitudinal and lateral aerodynamic angles of attack are computed using equation (8).

$$\alpha = \tan^{-1}\left(\frac{w}{u}\right) \text{ and } \beta = \tan^{-1}\left(\frac{v}{u}\right). \quad (8)$$

The aerodynamic coefficients in equation (7) are functions of local Mach number at the projectile mass center. They are computed using linear interpolation from a table of data. The aerodynamic forces and moments are assumed to act solely on the forward body.

The right side of the rotation kinetic equations contains the externally applied moments on both the forward and aft bodies. The external moment components on the forward body are given by equation (9) and contain contributions from steady (SA) and unsteady (UA) aerodynamics.

$$\begin{Bmatrix} L_A \\ M_A \\ N_A \end{Bmatrix} = \begin{Bmatrix} L_{SA} \\ M_{SA} \\ N_{SA} \end{Bmatrix} + \begin{Bmatrix} L_{UA} \\ M_{UA} \\ N_{UA} \end{Bmatrix}. \quad (9)$$

The steady body aerodynamic moment is computed by a cross between the distance vector from the center of gravity to the center of pressure, and the steady body aerodynamic force vector. The

The unsteady body aerodynamic moment provides a damping source for projectile angular motion and is given by equation (10).

$$\begin{Bmatrix} L_{UA} \\ M_{UA} \\ N_{UA} \end{Bmatrix} = q_a D^2 \begin{Bmatrix} C_{DD} + \frac{p_F DC_{LP}}{2V} \\ \frac{q DC_{MQ}}{2V} \\ \frac{r DC_{NR}}{2V} \end{Bmatrix}. \quad (10)$$

Air density is computed using the center of gravity position of the projectile using the standard atmosphere [2].

3. Simulation Example

In order to exercise the math model discussed previously, consider a 6-ft long, 120-lb projectile. The forward body is fin stabilized and the aft body is an internal circular cylinder. Aerodynamic forces and moments act on the forward body only. For this simulation set, initial forward body velocity is 750 m/s and initial gun elevation is 45°. All other states variables are initially equal to 0. The projectile fins are canted slightly to provide a slowly rolling projectile in steady state.

Figures 2–11 show the state variables of the system vs. time for the conditions mentioned above. The mass ratio of the aft body to the forward body is 1%. Under these circumstances, the projectile has a range of approximately 18 km. Cross range, yaw angle, side velocity, vertical velocity, pitch rate, yaw rate, and aerodynamic angle of attack remain small throughout the event. Pitch attitude steadily decreases from 45° to just below –60° at impact. Figures 2–11 remain the same, independent of the bearing resistance coefficient. Figures 12 and 13 show the roll angle and roll rate response as a function of bearing resistance coefficient. Values of bearing resistance coefficient are 0.000001, 0.000005, 0.00001, 0.00005, 0.0001, 0.0005, 0.001, 0.005,

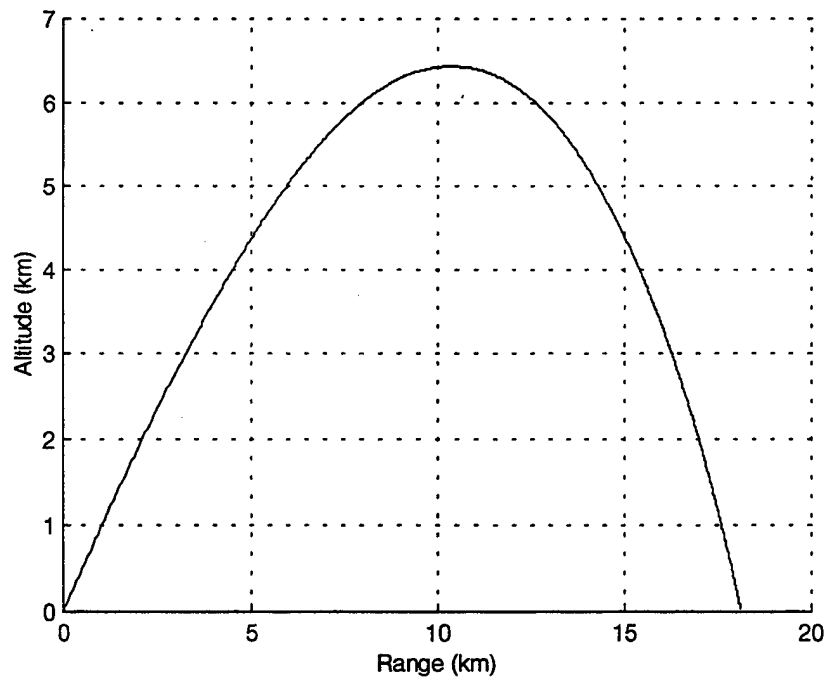


Figure 2. Range.

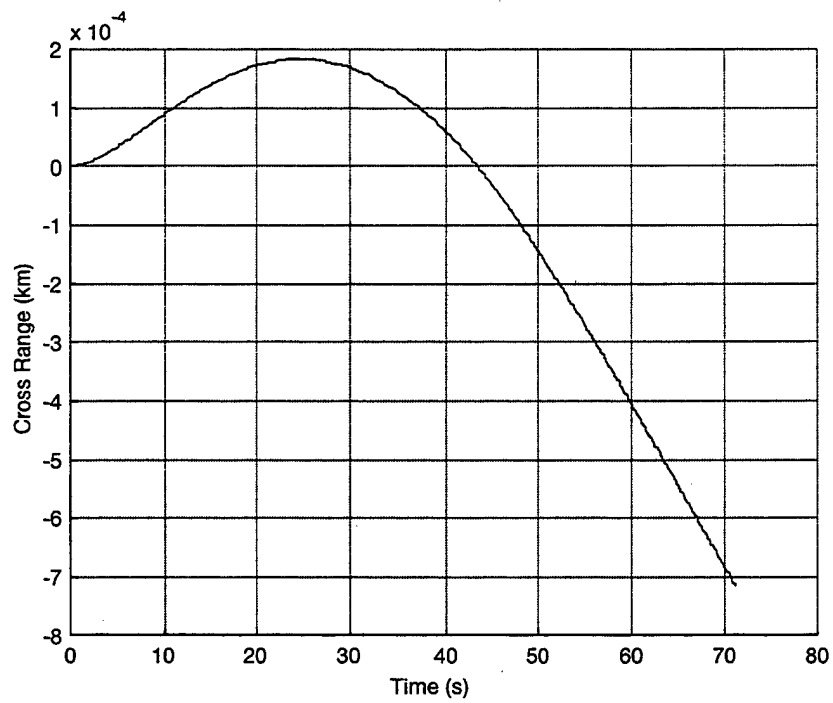


Figure 3. Cross Range.

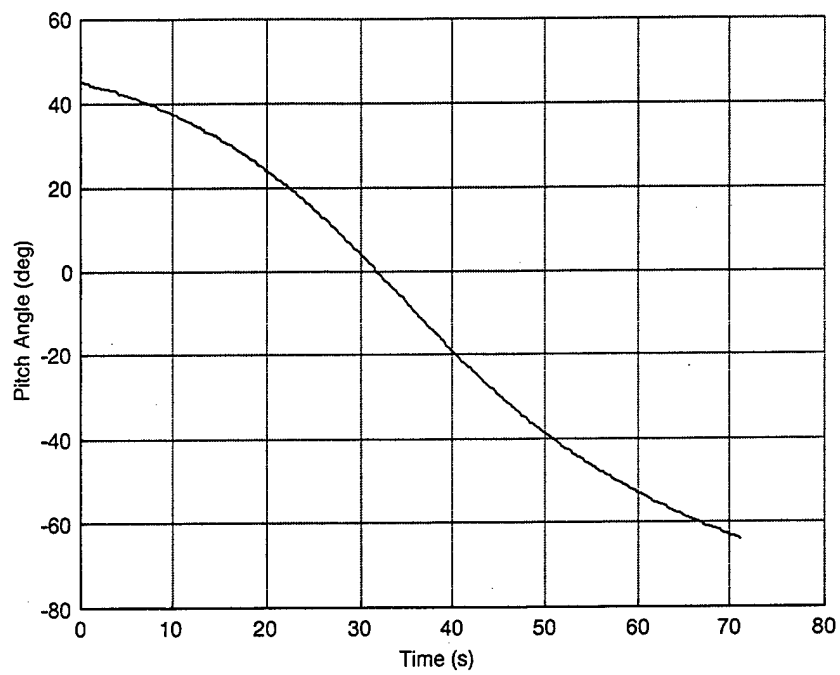


Figure 4. Euler Pitch Angle.

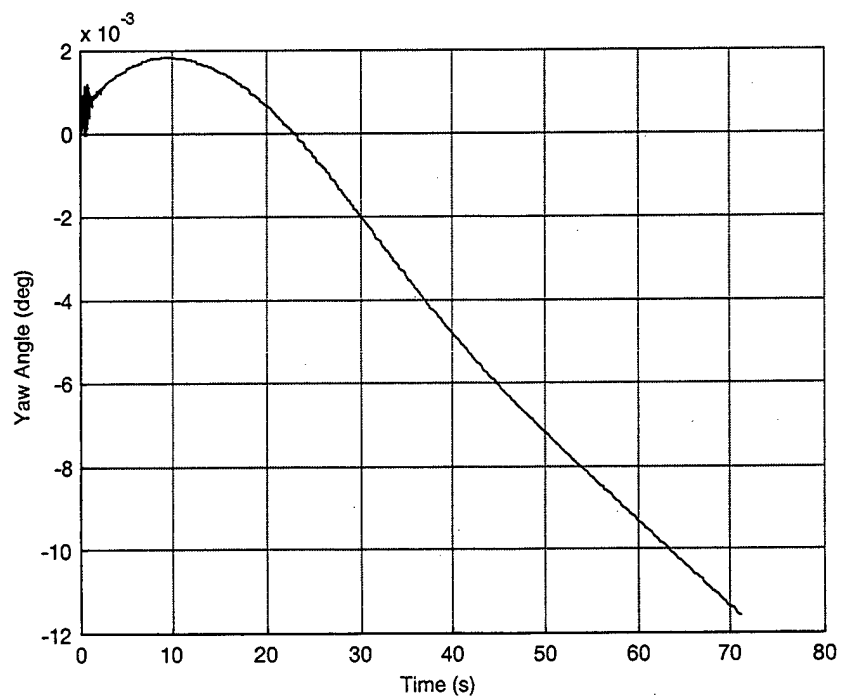


Figure 5. Euler Yaw Angle.

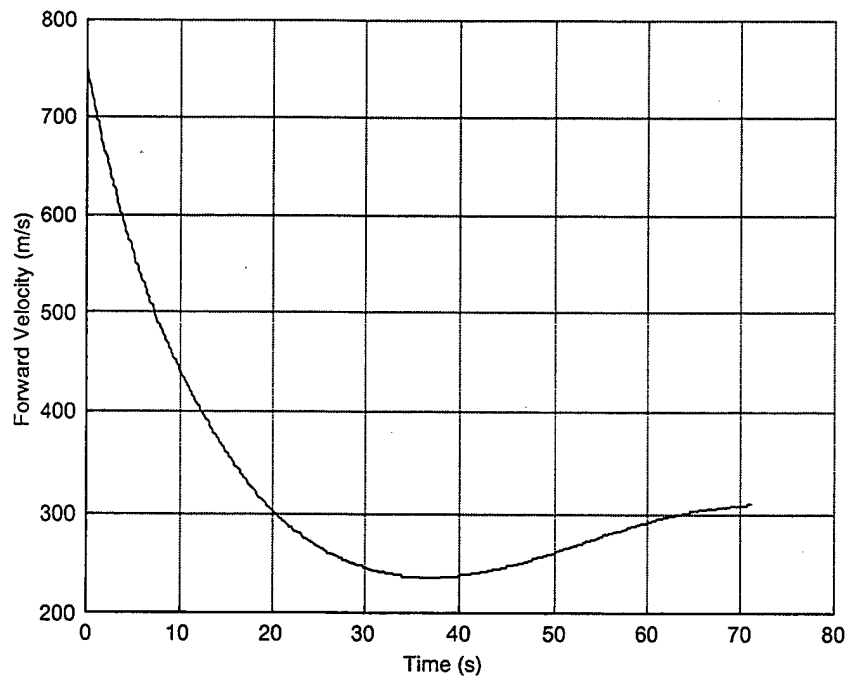


Figure 6. Forward Body Velocity.

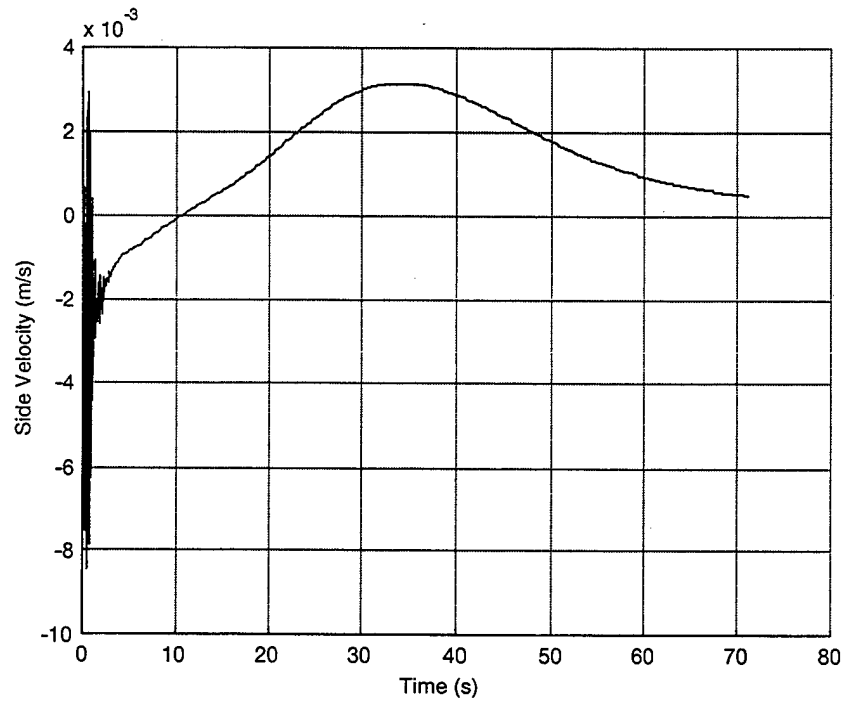


Figure 7. Side Body Velocity.

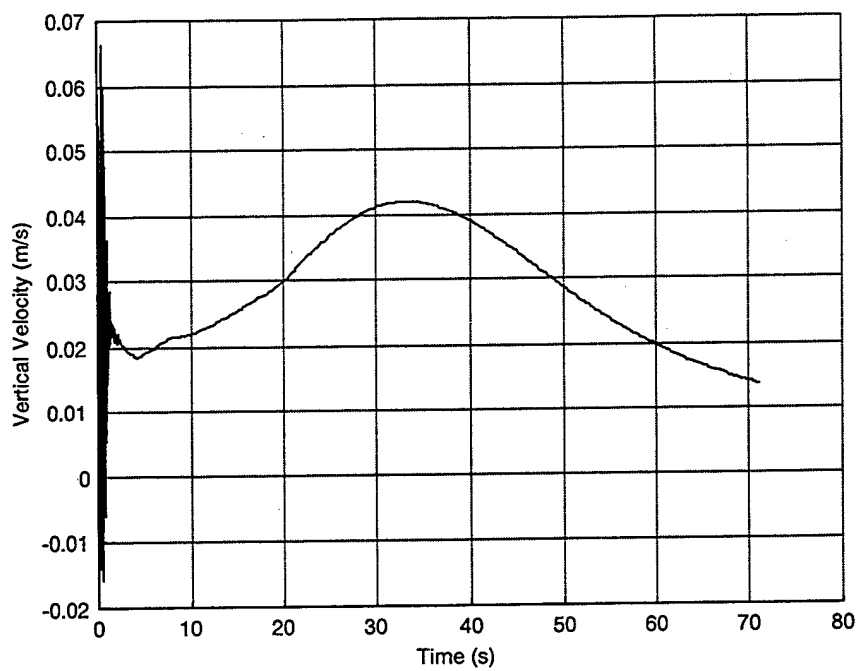


Figure 8. Vertical Body Velocity.

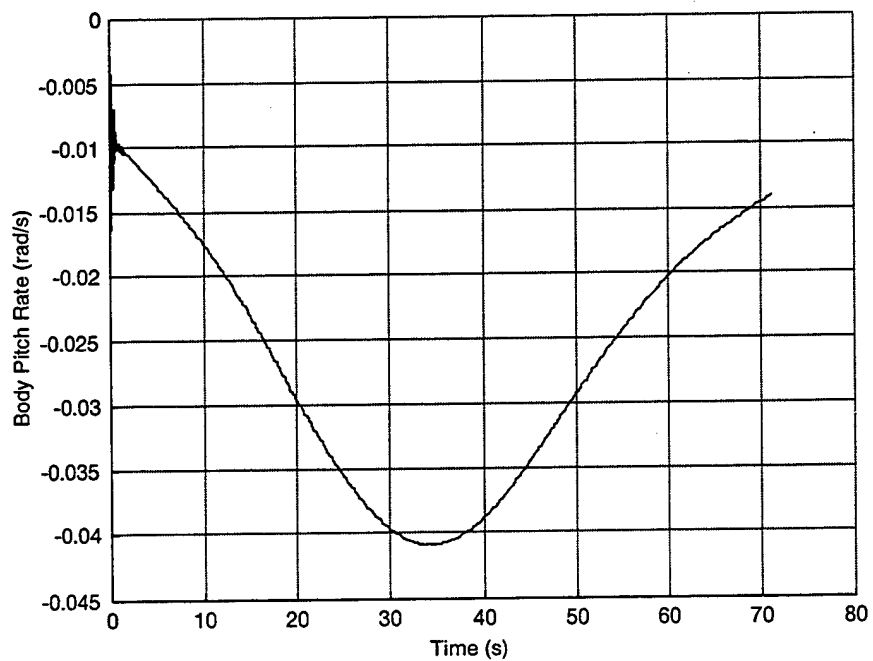


Figure 9. Pitch Rate.

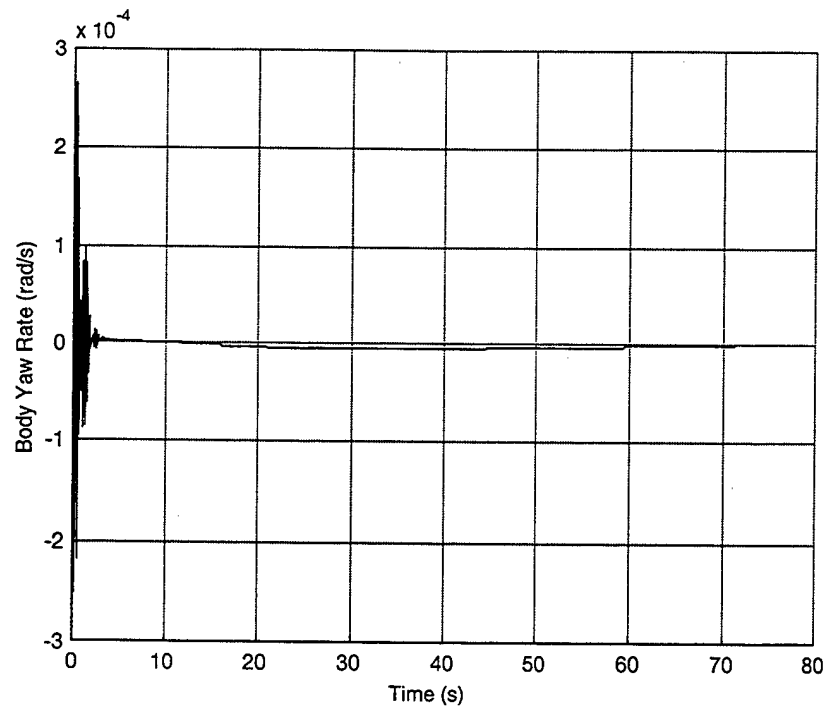


Figure 10. Yaw Rate.

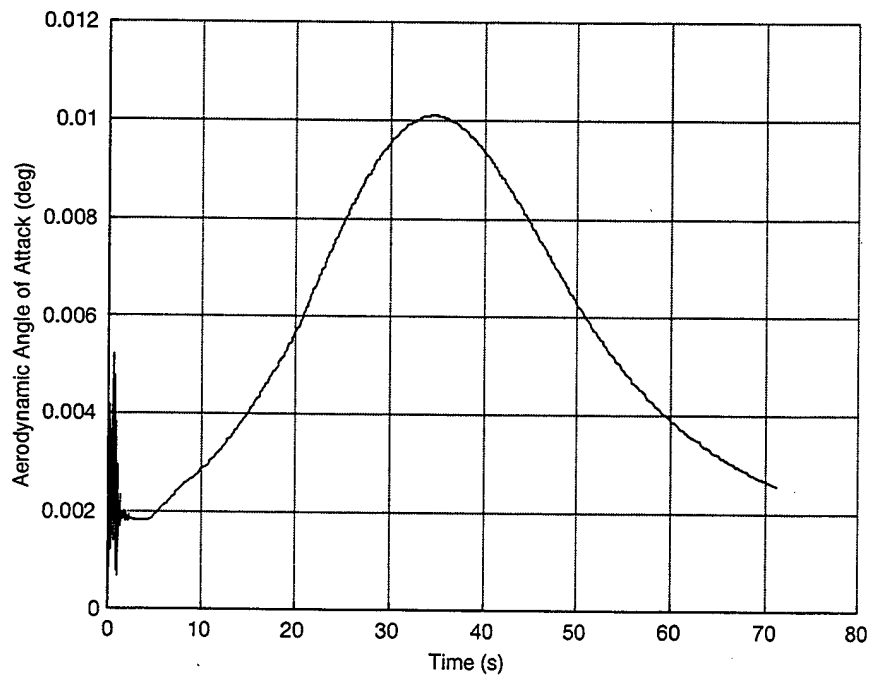


Figure 11. Aerodynamic Angle of Attack.

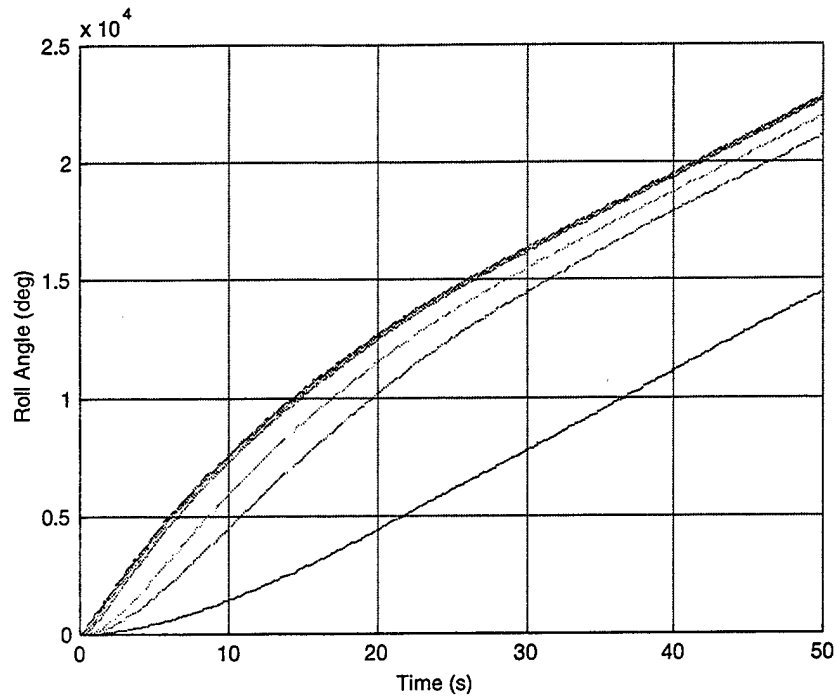


Figure 12. Roll Angle (Mass Ratio = 1%, Damping Coefficient = 0.01–0.000001).

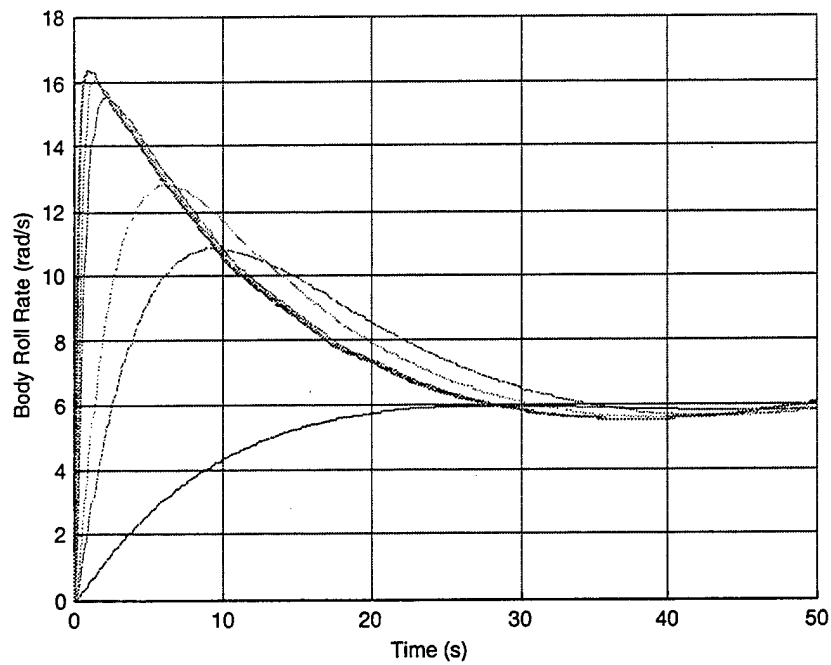


Figure 13. Roll Rate (Mass Ratio = 1%, Damping Coefficient = 0.01–0.000001).

and 0.01 ft-lbf/rps. In Figure 12, the lowest trace is the response of the aft body for the lowest value of bearing resistance. The upper trace is the forward body roll response. For a bearing resistance coefficient of 0.00005, the aft body roll response is essentially the same as the forward body since both bodies rapidly couple in the roll axis. Figure 13 shows the roll rate trace for this simulation set. It is interesting that for lower values of bearing resistance, the aft body roll rate overshoots the forward body roll rate before settling.

Figures 14 and 15 show the roll angle and roll rate response of forward and aft bodies under the same conditions as the previous case, except the mass ratio is now 50% rather than 1%. While the basic character of the roll response is the same, the aft body roll angle, and hence roll rate, build up relatively slowly due to the increase in aft body inertia.

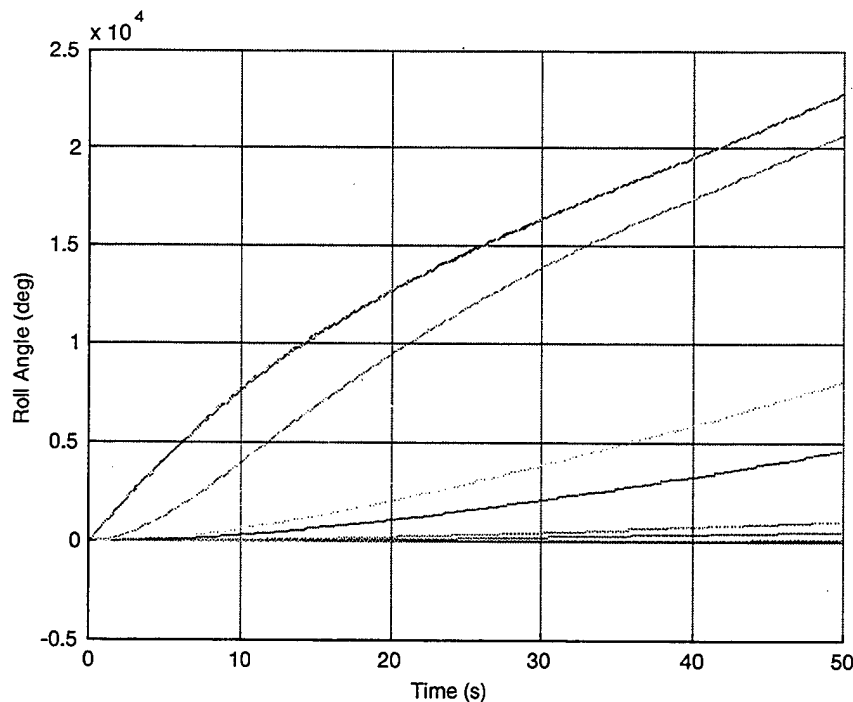


Figure 14. Roll Angle (Mass Ratio = 50%, Damping Coefficient = 0.01–0.000001).

Figures 16–19 show the response of the system under the same conditions as Figures 14 and 15, except the initial roll rate of the aft body is -100 rad/s. Like the previous simulation results,

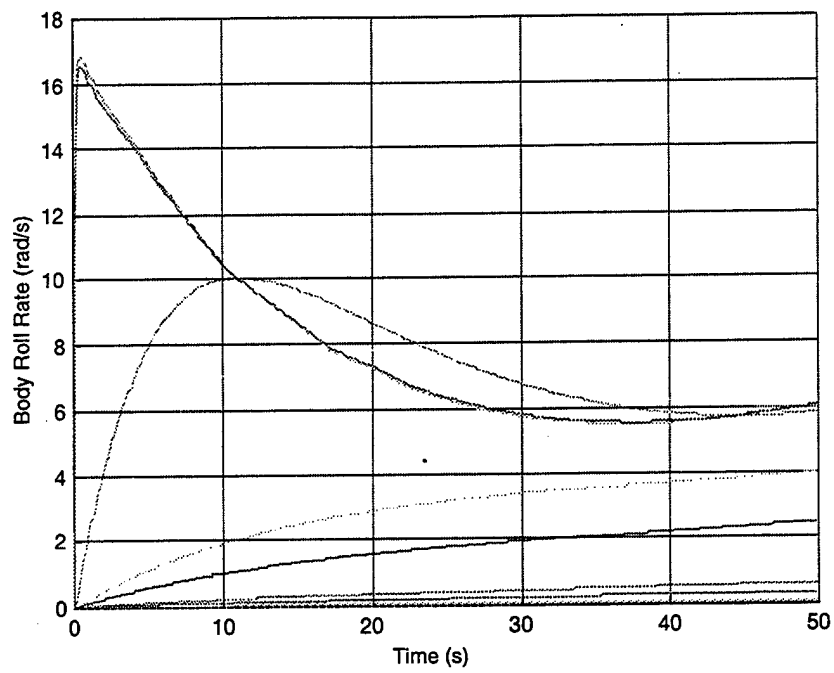


Figure 15. Roll Rate (Mass Ratio = 50%, Damping Coefficient = 0.01–0.000001).

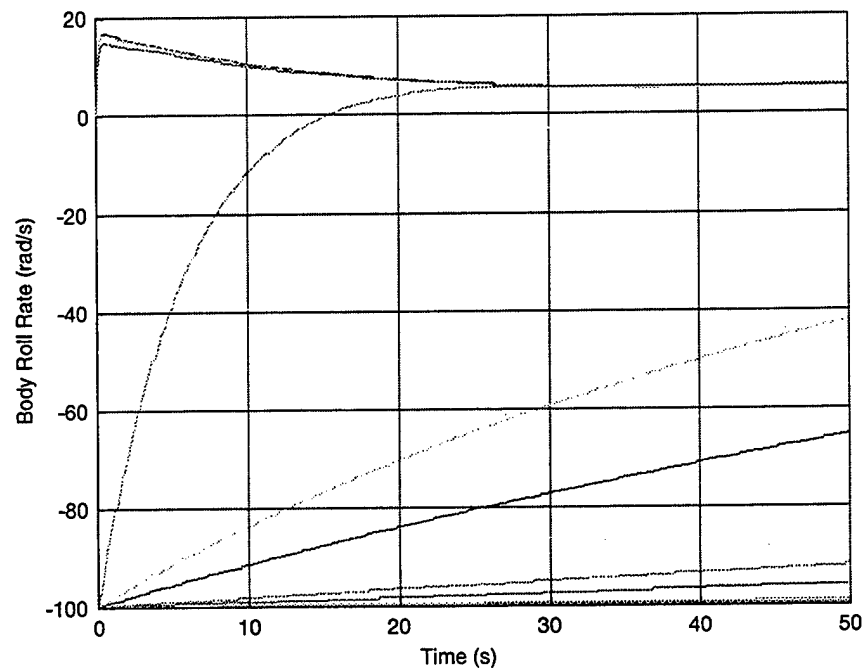


Figure 16. Roll Rate (Mass Ratio = 50%, Damping Coefficient = 0.01–0.000001).

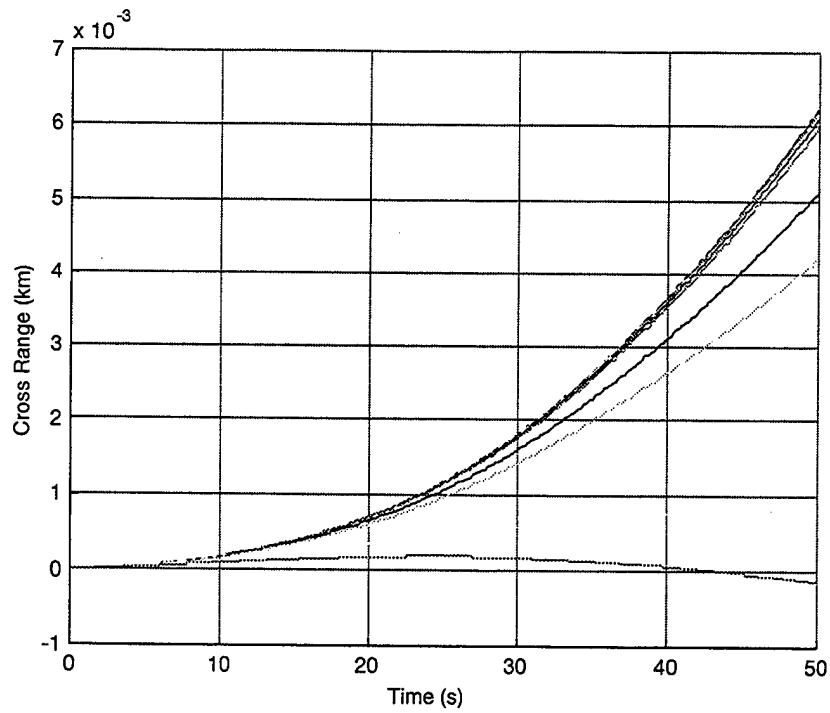


Figure 17. Cross Range (Mass Ratio = 50%, Damping Coefficient = 0.01–0.000001).

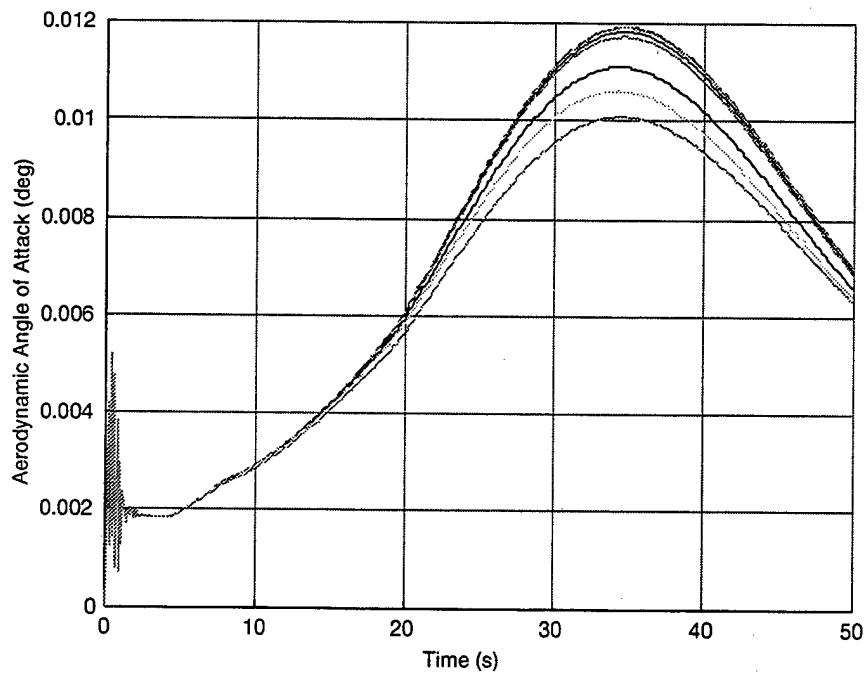


Figure 18. Angle of Attack (Mass Ratio = 50%, Damping Coefficient = 0.01–0.000001).

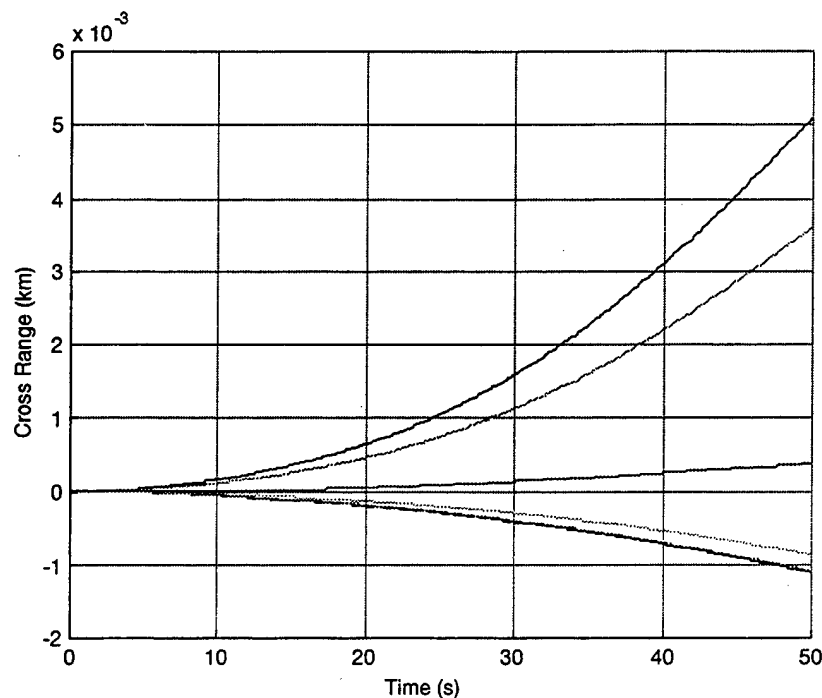


Figure 19. Cross Range (Damping Coefficient = 0.0005, Mass Ratio = 1%–50%).

lower values of bearing resistance produce slower roll response in the aft body. For larger splits in the forward and aft body roll rates, the trajectory begins to change as a function of bearing resistance owing to the fact that the roll response is sensitive to bearing resistance. In particular, Figure 17 shows the cross range under these circumstances. While the spray in the trajectory is only on the order of 10 m, it points to the fact that if the forward and aft bodies possess substantially different initial roll rates, the trajectory becomes a function of bearing resistance.

Figures 19–22 show system response under the same conditions as Figures 16–19, except now the mass ratio is varied. Figure 22 shows the roll rate response. Due to aft body inertia changes, the roll response varies significantly with mass ratio. Subsequently, the trajectory begins to vary as well. Similar to the previous case, the trajectory spray is on the order of 10 m; this shows that trajectory of configurations with forward and aft bodies operating at significantly different roll rates is a function of the mass ratio.

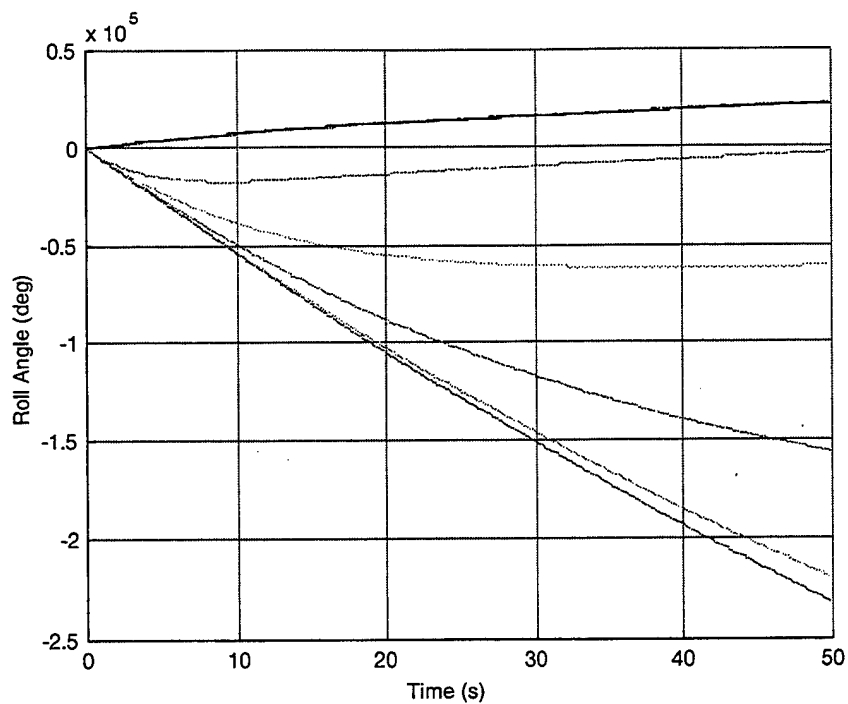


Figure 20. Roll Angle (Damping Coefficient = 0.0005, Mass Ratio = 1%–50%).

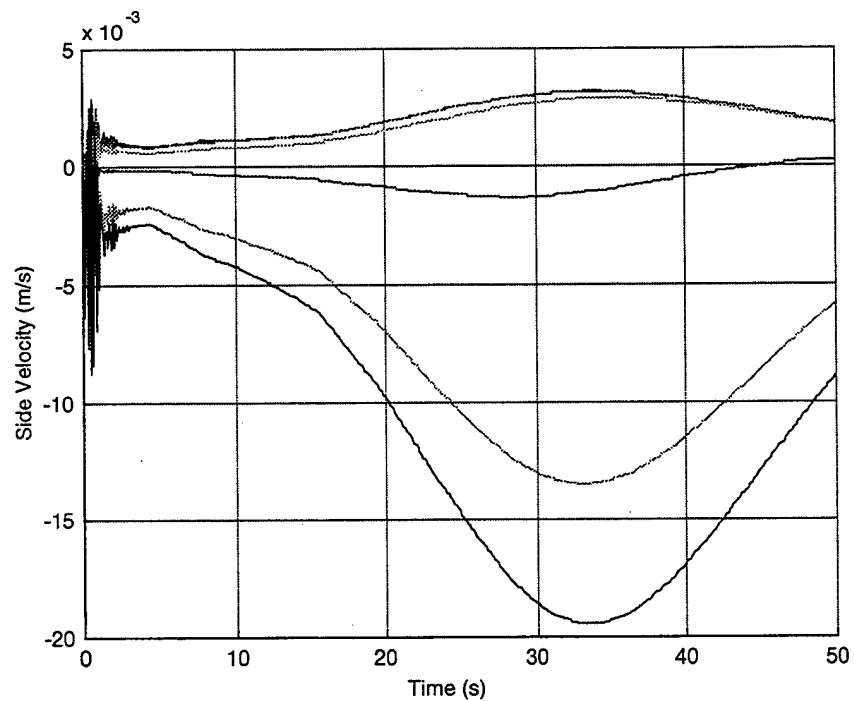


Figure 21. Side Velocity (Damping Coefficient = 0.0005, Mass Ratio = 1%–50%).

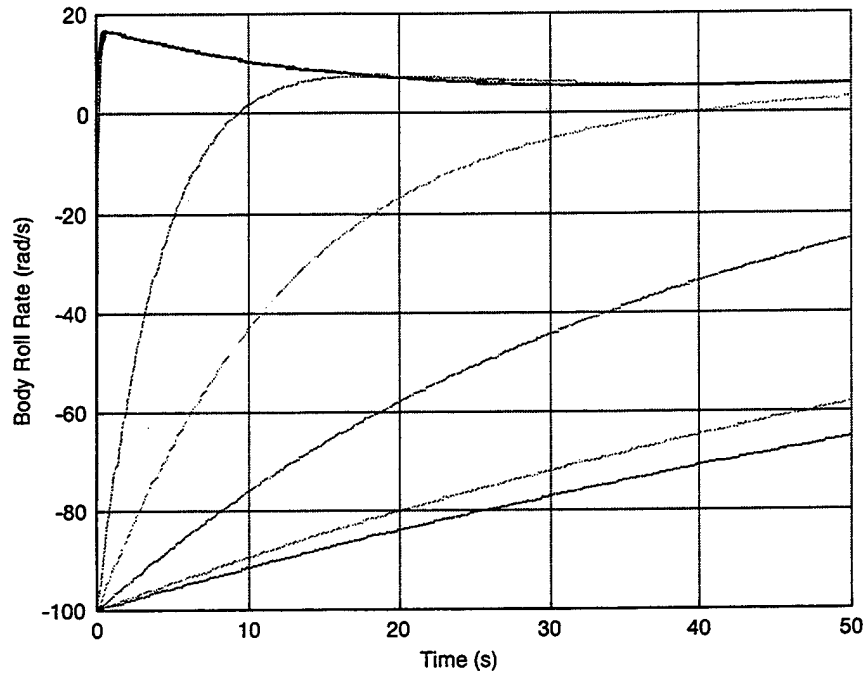


Figure 22. Roll Rate (Damping Coefficient = 0.0005, Mass Ratio = 1%–50%).

4. Conclusions

The equations of motion for a differential roll projectile configuration with seven degrees of freedom have been developed and exercised. The dynamic equations allow the forward and aft bodies to be mass unbalanced. A hydrodynamic bearing between the forward and aft components couples the roll degrees of freedom. Bearing resistance and forward/aft body mass ratio are the dominant factors in determining the roll dynamics. For spin rates typical of fin-stabilized projectiles, the trajectory is essentially independent of both bearing resistance and mass ratio. However, for configurations with the forward and aft components operating at significantly different roll rates, the trajectory depends on the mass ratio and bearing resistance.

INTENTIONALLY LEFT BLANK.

5. References

1. Etkin, B. *Dynamics of Atmospheric Flight*. New York: John Wiley and Sons, 1972.
2. Von Mises, R. *Theory of Flight*. New York: Dover Publications Inc., 1959.
3. Close, C. M., and D. K. Frederick. *Modeling and Analysis of Dynamic Systems*. New York: John Wiley and Sons, 1995.

INTENTIONALLY LEFT BLANK.

Appendix A:
Constraint Forces and Moments

INTENTIONALLY LEFT BLANK.

The rotation kinetic differential equations are derived by first splitting the two body system at the bearing connection point. Figures A-1 and A-2 show the external loads and internal constraint forces acting on both the forward and aft bodies, respectively.

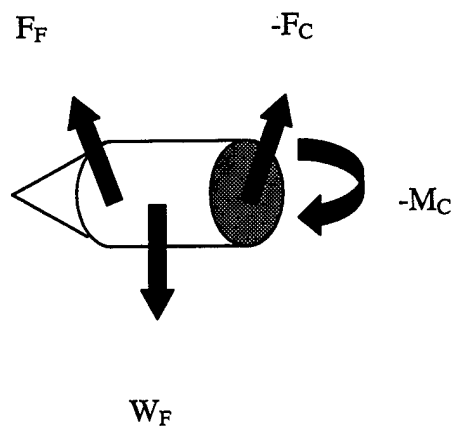


Figure A-1. Forces and Moments on the Forward Body.

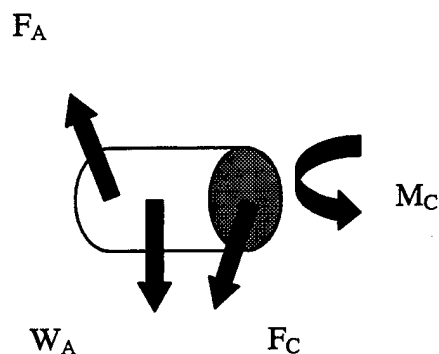


Figure A-2. Forces and Moments on the Aft Body.

The constraint force, F_C , and the constraint moment, M_C , couple the forward and aft bodies. Key to the development of the rotation kinetic differential equations is the ability to solve for the constraint forces and moments as a function of state variables and time derivatives of state variables.

An expression for the constraint force can be obtained by subtracting the translation dynamic equations for both bodies.

$$\frac{m}{m_F m_A} \bar{F}_C = \frac{\bar{F}_F}{m_F} - \frac{\bar{F}_A}{m_A} + \bar{a}_{A/I} - \bar{a}_{F/I}. \quad (\text{A-1})$$

The acceleration of the mass center of the forward and aft bodies, $\bar{a}_{F/I}$ and $\bar{a}_{A/I}$, can be expressed in terms of the acceleration of the composite body mass center. After making this substitution, the constraint force components in the fixed-plane reference frame can be expressed in the following manner:

$$\begin{Bmatrix} F_{CX} \\ F_{CY} \\ F_{CZ} \end{Bmatrix} = [\bar{F}_F] \begin{Bmatrix} \dot{p}_F \\ \dot{q} \\ \dot{r} \end{Bmatrix} + [\bar{F}_A] \begin{Bmatrix} \dot{p}_A \\ \dot{q} \\ \dot{r} \end{Bmatrix} + \{\bar{F}_0\}. \quad (\text{A-2})$$

The matrices $[\bar{F}_F]$, $[\bar{F}_A]$, and $\{\bar{F}_0\}$ are complicated functions of the state variables and the geometry of the configuration.

The components in the fixed-plane reference frame of the moment of the constraint force, acting on the forward body about the forward body mass center, can be written in the following manner:

$$\begin{Bmatrix} M_{FCFX} \\ M_{FCFY} \\ M_{FCFZ} \end{Bmatrix} = [\bar{M}_{FF}] \begin{Bmatrix} \dot{p}_F \\ \dot{q} \\ \dot{r} \end{Bmatrix} + [\bar{M}_{FA}] \begin{Bmatrix} \dot{p}_A \\ \dot{q} \\ \dot{r} \end{Bmatrix} + \{\bar{M}_{F0}\}. \quad (\text{A-3})$$

In a similar way, the components in the fixed-plane reference frame of the moment of the constraint force, acting on the aft body about the aft body mass center, can be written in the following manner:

$$\begin{Bmatrix} M_{FC_{AX}} \\ M_{FC_{AY}} \\ M_{FC_{AZ}} \end{Bmatrix} = [\overline{M}_{AF}] \begin{Bmatrix} \dot{p}_F \\ \dot{q} \\ \dot{r} \end{Bmatrix} + [\overline{M}_{AA}] \begin{Bmatrix} \dot{p}_A \\ \dot{q} \\ \dot{r} \end{Bmatrix} + \{\overline{M}_{A0}\}. \quad (\text{A-4})$$

The matrices $[\overline{M}_{FF}]$, $[\overline{M}_{FA}]$, $[\overline{M}_{AA}]$, $[\overline{M}_{AF}]$, $\{\overline{M}_{F0}\}$, and $\{\overline{M}_{A0}\}$ are also complicated functions of the state variables and the geometry of the configuration.

INTENTIONALLY LEFT BLANK.

Appendix B:
Rotation Kinetic Equations

INTENTIONALLY LEFT BLANK.

The rotation kinetic differential equations are derived by first writing the Euler equations for the forward and aft bodies separately. These equations are expressed in the fixed-plane reference frame are general, and allow for a fully populated inertia matrix and mass unbalance. Equations (A-2), (A-3), and (A-4) are substituted into both sets of rotation kinetic equations for the forward and aft bodies. At this point, both sets of equations still have unknown constraint moments at the bearing connection point. To eliminate the bearing constraint moments in the y and z direction in the fixed-plane coordinate system, the y and z components of the rotation kinetic equations for the forward and aft bodies are added together to form two dynamic equations that are free of constraint moments. In this way, the constraint moments at the bearing have been eliminated analytically.

The forward and aft bodies are connected through a hydrodynamic bearing. The moment transmitted across a hydrodynamic bearing can be modeled as viscous damping.¹ The constitutive relation governing the constraint moment transmitted across a hydrodynamic bearing is given by Equation (B-1).

$$M_V = c_V (p_F - p_A). \quad (B-1)$$

If the viscous damping coefficient, c_V , equals zero, then the forward and aft body connection is frictionless.

The effective inertia matrix is a 4×4 matrix that is a combination of the inertia matrices of both the forward and aft bodies. As an aid in developing a formula for the effective inertia matrix, define the following intermediate matrices:

$$[I_{FF}] = [I_F]^T [I_F] + [\bar{M}_{FF}], \quad (B-2)$$

¹ Close, C. M., and D. K. Frederick. *Modeling and Analysis of Dynamic Systems*. New York: John Wiley and Sons, 1995.

$$[I_{FA}] = [\overline{M}_{FA}], \quad (B-3)$$

$$[I_{AA}] = [T_A]^T [I_A] [T_A] - [\overline{M}_{AA}], \text{ and} \quad (B-4)$$

$$[I_{AF}] = -[\overline{M}_{AF}]. \quad (B-5)$$

Using Equations (B-2), (B-3), (B-4), and (B-5), elements of the effective inertia matrix can now be formed.

$$I_{1,1} = I_{FF_{1,1}}, \quad (B-6)$$

$$I_{1,2} = I_{FA_{1,1}}, \quad (B-7)$$

$$I_{1,3} = I_{FF_{1,2}} + I_{FA_{1,2}}, \quad (B-8)$$

$$I_{1,4} = I_{FF_{1,3}} + I_{FA_{1,3}}, \quad (B-9)$$

$$I_{2,1} = I_{AF_{1,1}}, \quad (B-10)$$

$$I_{2,2} = I_{AA_{1,1}}, \quad (B-11)$$

$$I_{2,3} = I_{AA_{1,2}} + I_{AF_{1,2}}, \quad (B-12)$$

$$I_{2,4} = I_{AA_{1,3}} + I_{AF_{1,3}}, \quad (B-13)$$

$$I_{3,1} = I_{FF_{2,1}} + I_{AF_{2,1}}, \quad (B-14)$$

$$I_{3,2} = I_{AA_{2,1}} + I_{FA_{2,1}}, \quad (\text{B-15})$$

$$I_{3,3} = I_{FF_{2,2}} + I_{AA_{2,2}} + I_{FA_{2,2}} + I_{AF_{2,2}}, \quad (\text{B-16})$$

$$I_{3,4} = I_{FF_{2,3}} + I_{AA_{2,3}} + I_{FA_{2,3}} + I_{AF_{2,3}}, \quad (\text{B-17})$$

$$I_{4,1} = I_{FF_{3,1}} + I_{AF_{3,1}}, \quad (\text{B-18})$$

$$I_{4,2} = I_{AA_{3,1}} + I_{FA_{3,1}}, \quad (\text{B-19})$$

$$I_{4,3} = I_{FF_{3,2}} + I_{AA_{3,2}} + I_{FA_{3,2}} + I_{AF_{3,2}}, \text{ and} \quad (\text{B-20})$$

$$I_{4,4} = I_{FF_{3,3}} + I_{AA_{3,3}} + I_{FA_{3,3}} + I_{AF_{3,3}}. \quad (\text{B-21})$$

The elements of the right-hand side vector are given by Equations (B-22) and (B-23).

$$\begin{Bmatrix} g_{F_1} \\ g_{F_2} \\ g_{F_3} \end{Bmatrix} = \begin{Bmatrix} M_{FX} \\ M_{FY} \\ M_{FZ} \end{Bmatrix} - [\bar{S}_F] \begin{Bmatrix} p_F \\ q \\ r \end{Bmatrix} - \{\bar{M}_{F0}\}, \text{ and} \quad (\text{B-22})$$

$$\begin{Bmatrix} g_{A_1} \\ g_{A_2} \\ g_{A_3} \end{Bmatrix} = \begin{Bmatrix} M_{AX} \\ M_{AY} \\ M_{AZ} \end{Bmatrix} - [\bar{S}_A] \begin{Bmatrix} p_A \\ q \\ r \end{Bmatrix} + \{\bar{M}_{A0}\}. \quad (\text{B-23})$$

The matrices $[\bar{S}_F]$ and $[\bar{S}_A]$ in Equations (B-22) and (B-23) are given by Equations (B-24) and (B-25) as follows:

$$[\bar{S}_F] = [T_F]^T [I_F] [\dot{T}_F] + [T_F]^T [S_F] [I_F] [T_F], \text{ and} \quad (\text{B-24})$$

$$[\bar{S}_A] = [T_A]^T [I_A] [\dot{T}_A] + [T_A]^T [S_A] [I_A] [T_A], \quad (\text{B-25})$$

where

$$[S_F] = \begin{bmatrix} 0 & s_{\phi_F} q - c_{\phi_F} r & c_{\phi_F} q + s_{\phi_F} r \\ c_{\phi_F} r - s_{\phi_F} q & 0 & -p_F \\ -c_{\phi_F} q - s_{\phi_F} r & p_F & 0 \end{bmatrix}, \quad (\text{B-26})$$

$$[S_A] = \begin{bmatrix} 0 & s_{\phi_A} q - c_{\phi_A} r & c_{\phi_A} q + s_{\phi_A} r \\ c_{\phi_A} r - s_{\phi_A} q & 0 & -p_A \\ -c_{\phi_A} q - s_{\phi_A} r & p_A & 0 \end{bmatrix}, \quad (\text{B-27})$$

$$[T_F] = \begin{bmatrix} 1 & 0 & 0 \\ 0 & c_{\phi_F} & s_{\phi_F} \\ 0 & -s_{\phi_F} & c_{\phi_F} \end{bmatrix}, \quad (\text{B-28})$$

$$[T_A] = \begin{bmatrix} 1 & 0 & 0 \\ 0 & c_{\phi_A} & s_{\phi_A} \\ 0 & -s_{\phi_A} & c_{\phi_A} \end{bmatrix}, \quad (\text{B-29})$$

$$[\dot{T}_F] = \begin{bmatrix} 0 & 0 & 0 \\ 0 & -(p_F + t_\theta r) s_{\phi_F} & (p_F + t_\theta r) c_{\phi_F} \\ 0 & -(p_F + t_\theta r) c_{\phi_F} & -(p_F + t_\theta r) s_{\phi_F} \end{bmatrix}, \text{ and} \quad (\text{B-30})$$

$$[\dot{T}_A] = \begin{bmatrix} 0 & 0 & 0 \\ 0 & -(p_A + t_\theta r) s_{\phi_A} & (p_A + t_\theta r) c_{\phi_A} \\ 0 & -(p_A + t_\theta r) c_{\phi_A} & -(p_A + t_\theta r) s_{\phi_A} \end{bmatrix}. \quad (\text{B-31})$$

List of Symbols

x, y, z	Position vector components of the center of mass expressed in the inertial reference frame
θ, ψ	Euler pitch, yaw angles
ϕ_F	Euler roll angle of the forward body
ϕ_A	Euler roll angle of the aft body
u, v, w	Translation velocity components of the center of mass resolved in the fixed-plane reference frame
p_F	Roll axis component of the angular velocity vector of the forward body expressed in the fixed-plane reference frame
p_A	Roll axis component of the angular velocity vector of the aft body expressed in the fixed-plane reference frame
q, r	Components of the angular velocity vector of both the forward and aft bodies expressed in the fixed-plane reference frame
X, Y, Z	Total external force components on the projectile expressed in the fixed-plane reference frame
L_F, M_F, N_F	External moments on the forward body expressed in the fixed-plane reference frame
L_A, M_A, N_A	External moments on the aft body expressed in the fixed plane reference frame
m_F	Forward body mass
m_A	Aft body mass
m	Total projectile mass
$[I_F]$	Mass moment of inertia matrix of the forward body with respect to the forward body reference frame
$[I_A]$	Mass moment of inertia matrix of the aft body with respect to the aft body reference frame
$[I]$	Effective inertia matrix
D	Projectile characteristic length
C_i	Projectile aerodynamic coefficients
q_a	Dynamic pressure at the projectile mass center
α	Longitudinal aerodynamic angle of attack
β	Lateral aerodynamic angle of attack
$[T_F]$	Transformation matrix from the fixed-plane reference frame to the forward body reference frame
$[T_A]$	Transformation matrix from the fixed-plane reference frame to the aft body reference frame
c_v	Viscous damping coefficient
V	Magnitude-of-mass center velocity

INTENTIONALLY LEFT BLANK.

<u>NO. OF COPIES</u>	<u>ORGANIZATION</u>
2	DEFENSE TECHNICAL INFORMATION CENTER DTIC DDA 8725 JOHN J KINGMAN RD STE 0944 FT BELVOIR VA 22060-6218
1	HQDA DAMO FDT 400 ARMY PENTAGON WASHINGTON DC 20310-0460
1	OSD OUSD(A&T)/ODDDR&E(R) R J TREW THE PENTAGON WASHINGTON DC 20301-7100
1	DPTY CG FOR RDA US ARMY MATERIEL CMD AMCRDA 5001 EISENHOWER AVE ALEXANDRIA VA 22333-0001
1	INST FOR ADVNCD TCHNLGY THE UNIV OF TEXAS AT AUSTIN PO BOX 202797 AUSTIN TX 78720-2797
1	DARPA B KASPAR 3701 N FAIRFAX DR ARLINGTON VA 22203-1714
1	NAVAL SURFACE WARFARE CTR CODE B07 J PENNELLA 17320 DAHLGREN RD BLDG 1470 RM 1101 DAHLGREN VA 22448-5100
1	US MILITARY ACADEMY MATH SCI CTR OF EXCELLENCE DEPT OF MATHEMATICAL SCI MADN MATH THAYER HALL WEST POINT NY 10996-1786

<u>NO. OF COPIES</u>	<u>ORGANIZATION</u>
1	DIRECTOR US ARMY RESEARCH LAB AMSRL D D R SMITH 2800 POWDER MILL RD ADELPHI MD 20783-1197
1	DIRECTOR US ARMY RESEARCH LAB AMSRL DD 2800 POWDER MILL RD ADELPHI MD 20783-1197
1	DIRECTOR US ARMY RESEARCH LAB AMSRL CS AS (RECORDS MGMT) 2800 POWDER MILL RD ADELPHI MD 20783-1145
3	DIRECTOR US ARMY RESEARCH LAB AMSRL CI LL 2800 POWDER MILL RD ADELPHI MD 20783-1145
	<u>ABERDEEN PROVING GROUND</u>
4	DIR USARL AMSRL CI LP (BLDG 305)

<u>NO. OF COPIES</u>	<u>ORGANIZATION</u>
3	AIR FORCE RSRCH LAB MUNITIONS DIR AFRL/MNAV G ABATE 101 W EGLIN BLVD STE 219 EGLIN AFB FL 32542
3	ALLEN PETERSON 159 S HIGHLAND DR KENNEWICK WA 99337
1	CDR WL/MNMF D MABRY 101 W EGLIN BLVD STE 219 EGLIN AFB FL 32542-6810
20	DEPT OF MECHL ENGRG M COSTELLO OREGON STATE UNIVERSITY CORVALLIS OR 97331
4	CDR US ARMY ARDEC AMSTA AR CCH J DELORENZO S MUSALI R SAYER P DONADIO PICATINNY ARESENAL NJ 07806-5000
7	CDR US ARMY TANK MAIN ARMAMENT SYSTEM AMCPM TMA D GUZIEWICZ R DARCEY C KIMKER R JOINSON E KOPOAC T LOUZIERIO C LEVECHIA PICATINNY ARESENAL NJ 07806-5000
1	CDR USA YUMA PROV GRND STEYT MTW YUMA AZ 85365-9103

<u>NO. OF COPIES</u>	<u>ORGANIZATION</u>
10	CDR US ARMY TACOM AMCPEO HFM AMCPEO HFM F AMCPEO HFM C AMCPM ABMS AMCPM BLOCKIII AMSTA CF AMSTA Z AMSTA ZD AMCPM ABMS S W DR PATTISON A HAVERILLA WARREN MI 48397-5000
1	DIR BENET LABORATORIES SMCWV QAR T MCCLOSKEY WATERVLIET NY 12189-5000
1	CDR USAOTEA CSTE CCA DR RUSSELL ALEXANDRIA VA 22302-1458
2	DIR US ARMY ARMOR CTR & SCHL ATSB WP ORSA A POMEY ATSB CDC FT KNOX KY 40121
1	CDR US ARMY AMCCOM AMSMC ASR A MR CRAWFORD ROCK ISLAND IL 61299-6000
2	PROGRAM MANAGER GROUND WEAPONS MCRDAC LTC VARELA CBGT QUANTICO VA 22134-5000

NO. OF
COPIES ORGANIZATION

4 COMMANDER
US ARMY TRADOC
ATCD T
ATCD TT
ATTE ZC
ATTG Y
FT MONROE VA 23651-5000

1 NAWC
F PICKETT
CODE C2774 CLPL
BLDG 1031
CHINA LAKE CA 93555

1 NAVAL ORDNANCE STATION
ADVNC D SYS TCHNLGY BRNCH
D HOLMES
CODE 2011
LOUISVILLE KY 40214-5001

1 NAVAL SURFACE WARFARE CTR
F G MOORE
DAHLGREN DIVISION
CODE G04
DAHLGREN VA 22448-5000

1 US MILITARY ACADEMY
MATH SCI CTR OF EXCELLENCE
DEPT OF MATHEMATICAL SCI
MDN A MAJ DON ENGEN
THAYER HALL
WEST POINT NY 10996-1786

3 DIR
SNL
A HODAPP
W OBERKAMPF
F BLOTTNER
DIVISION 1631
ALBUQUERQUE NM 87185

3 ALLIANT TECH SYSTEMS
C CANDLAND
R BURETTA
R BECKER
7225 NORTHLAND DR
BROOKLYN PARK MN 55428

NO. OF
COPIES ORGANIZATION

3 DIR USARL
AMSRL SE RM
H WALLACE
AMSRL SS SM
J EIKE
A LADAS
2800 POWDER MILL RD
ADELPHI MD 20783-1145

1 OFC OF ASST SECY OF ARMY
FOR R&D
SARD TR
W MORRISON
2115 JEFFERSON DAVIS HWY
ARLINGTON VA 22202-3911

2 CDR USARDEC
AMSTA FSP A
S DEFEO
R SICIGNANO
PICATINNY ARESENAL NJ
07806-5000

2 CDR USARDEC
AMSTA AR CCH A
M PALATHINGAL
R CARR
PICATINNY ARESENAL NJ
07806-5000

5 TACOM ARDEC
AMSTA AR FSA
K CHIEFA
AMSTA AR FS
A WARNASCH
AMSTA AR FSF
W RYBA
AMSTA AR FSP
S PEARCY
J HEDDERICH
PICATINNY ARESENAL NJ
07806-5000

<u>NO. OF</u> <u>COPIES</u>	<u>ORGANIZATION</u>
5	CDR US ARMY MICOM AMSMI RD P JACOBS P RUFFIN AMSMI RD MG GA C LEWIS AMSMI RD MG NC C ROBERTS AMSMI RD ST GD D DAVIS RSA AL 35898-5247
3	CDR US ARMY AVN TRP CMD DIRECTORATE FOR ENGINEERING AMSATR ESW M MAMOUD M JOHNSON J OBERMARK RSA AL 35898-5247
1	DIR US ARMY RTTC STERT TE F TD R EPPS BLDG 7855 RSA AL 35898-8052
2	STRICOM AMFTI EL D SCHNEIDER R COLANGELO 12350 RESEARCH PKWY ORLANDO FL 32826-3276
1	CDR OFFICE OF NAVAL RES CODE 333 J GOLDWASSER 800 N QUINCY ST RM 507 ARLINGTON VA 22217-5660
1	CDR US ARMY RES OFFICE AMXRO RT IP TECH LIB PO BOX 12211 RESEARCH TRIANGLE PARK NJ 27709-2211

<u>NO. OF</u> <u>COPIES</u>	<u>ORGANIZATION</u>
4	CDR US ARMY AVN TRP CMD AVIATION APPLIED TECH DIR AMSATR TI R BARLOW E BERCHER T CONDON B TENNEY FT EUSTIS VA 23604-5577
3	CDR NAWC WEAPONS DIV CODE 543400D S MEYERS CODE C2744 T MUNSINGER CODE C3904 D SCOFIELD CHINA LAKE CA 93555-6100
1	CDR NSWC CRANE DIVISION CODE 4024 J SKOMP 300 HIGHWAY 361 CRANE IN 47522-5000
1	CDR NSWC DAHLGREN DIV CODE 40D J BLANKENSHIP 6703 WEST HWY 98 PANAMA CITY FL 32407-7001
1	CDR NSWC J FRAYSEE D HAGEN 17320 DAHLGREN RD DAHLGREN VA 22448-5000

NO. OF
COPIES ORGANIZATION

5 CDR NSWC
INDIAN HEAD DIV
CODE 40D
D GARVICK
CODE 4110C
L FAN
CODE 4120
V CARLSON
CODE 4140E
H LAST
CODE 450D
T GRIFFIN
101 STRAUSS AVE
INDIAN HEAD MD 20640-5000

1 CDR NSWC
INDIAN HEAD DIV
LIBRARY CODE 8530
BLDG 299
101 STRAUSS AVE
INDIAN HEAD MD 20640

2 US MILITARY ACADEMY
MATH SCI CTR OF EXCELLENCE
DEPT OF MATHEMATICAL SCI
MDN A
MAJ D ENGEN
R MARCHAND
THAYER HALL
WEST POINT NY 10996-1786

3 CDR US ARMY YUMA PG
STEYP MT AT A
A HOOPER
STEYP MT EA
YUMA AZ 85365-9110

6 CDR NSWC
INDIAN HEAD DIV
CODE 570D J BOKSER
CODE 5710 L EAGLES
J FERSUSON
CODE 57 C PARIS
CODE 5710G S KIM
CODE 5710E S JAGO
101 STRAUSS AVE ELY BLDG
INDIAN HEAD MD 20640-5035

NO. OF
COPIES ORGANIZATION

1 BRUCE KIM
MICHIGAN STATE UNIVERSITY
2120 ENGINEERING BLDG
EAST LANSING MI 48824-1226

2 INDUSTRIAL OPERATION CMD
AMFIO PM RO
W MCKELVIN
MAJ BATEMAN
ROCK ISLAND IL 61299-6000

3 PROGRAM EXECUTIVE OFFICER
TACTICAL AIRCRAFT PROGRAMS
PMA 242 1
MAJ KIRBY R242
PMA 242 33
R KEISER (2 CPS)
1421 JEFFERSON DAVIS HWY
ARLINGTON VA 22243-1276

1 CDR NAVAL AIR SYSTEMS CMD
CODE AIR 471
A NAKAS
1421 JEFFERSON DAVIS HWY
ARLINGTON VA 22243-1276

4 ARROW TECH ASSOCIATES INC
R WHYTE
A HATHAWAY
H STEINHOFF
1233 SHELBOURNE RD SUITE D8
SOUTH BURLINGTON VT 05403

3 US ARMY AVIATION CTR
DIR OF COMBAT DEVELOPMENT
ATZQ CDM C
B NELSON
ATZQ CDC C
T HUNDLEY
ATZQ CD
G HARRISON
FORT RUCKER AL 36362

NO. OF
COPIES ORGANIZATION

ABERDEEN PROVING GROUND

3 CDR
USA ARDEC
AMSTA AR FSF T
R LIESKE
J WHITESIDE
J MATTS
BLDG 120

1 CDR
USA ATEC
CSTE CT
T J SCHNELL
RYAN BLDG

3 CDR
USA AMSAA
AMXSY EV
G CASTLEBURY
R MIRABELLE
AMXSY EF
S MCKEY

58 DIR USARL
AMSRL WM
I MAY
T ROSENBERGER
AMSRL WM BA
W HORST JR
W CIEPELLA
AMSRL WM BE
M SCHMIDT
AMSRL WM BA
F BRANDON
T BROWN (5 CPS)
L BURKE
J CONDON
B DAVIS
T HARKINS (5 CPS)
D HEPNER
V LEITZKE
M HOLLIS
A THOMPSON

NO. OF
COPIES ORGANIZATION

ABERDEEN PROVING GROUND (CONTD)

AMSRL WM BB
B HAUG
AMSRL WM BC
J GARNER
AMSRL WM BD
B FORCH
AMSRL WM BF
J LACETERA
P HILL
AMSRL WM BR
C SHOEMAKER
J BORNSTEIN
AMSRL WM BA
G BROWN
B DAVIS
T HARKINS
D HEPNER
A THOMPSON
J CONDON
W DAMICO
F BRANDON
AMSRL WM BC
P PLOSTINS (4 CPS)
G COOPER
B GUIDOS
J SAHU
M BUNDY
K SOENCKSEN
D LYON
A HORST
I MAY
J BENDER
J NEWILL
AMSRL WM BC
V OSKAY
S WILKERSON
W DRYSDALE
R COATES
A MIKHAL
J WALL

REPORT DOCUMENTATION PAGE			Form Approved OMB No. 0704-0188	
Public reporting burden for this collection of information is estimated to average 1 hour per response, including the time for reviewing instructions, searching existing data sources, gathering and maintaining the data needed, and completing and reviewing the collection of information. Send comments regarding this burden estimate or any other aspect of this collection of information, including suggestions for reducing this burden, to Washington Headquarters Services, Directorate for Information Operations and Reports, 1215 Jefferson Davis Highway, Suite 1204, Arlington, VA 22202-4302, and to the Office of Management and Budget, Paperwork Reduction Project (0704-0188), Washington, DC 20503.				
1. AGENCY USE ONLY (Leave blank)		2. REPORT DATE July 2000	3. REPORT TYPE AND DATES COVERED Final, Apr 98 - Apr 99	
4. TITLE AND SUBTITLE Modeling and Simulation of a Differential Roll Projectile			5. FUNDING NUMBERS DAAL01-98-M-0033	
6. AUTHOR(S) Mark F. Costello*				
7. PERFORMING ORGANIZATION NAME(S) AND ADDRESS(ES) Oregon State University Corvallis, OR 97331			8. PERFORMING ORGANIZATION REPORT NUMBER	
9. SPONSORING/MONITORING AGENCY NAME(S) AND ADDRESS(ES) U.S. Army Research Laboratory ATTN: AMSRL-WM-BC Aberdeen Proving Ground, MD 21005-5066			10. SPONSORING/MONITORING AGENCY REPORT NUMBER ARL-CR-455	
11. SUPPLEMENTARY NOTES Oregon State University Corvallis, OR 97331				
12a. DISTRIBUTION/AVAILABILITY STATEMENT Approved for public release; distribution is unlimited.			12b. DISTRIBUTION CODE	
13. ABSTRACT (Maximum 200 words) This report develops the equations of motion for a differential roll projectile configuration with seven degrees of freedom. The dynamic equations are generated generically such that the forward and aft components are mass unbalanced. A hydrodynamic bearing exists between the forward and aft components, which couples the roll degree of freedom. A simulation investigation shows that bearing resistance and forward/aft body mass ratio are the dominant factors in determining the roll dynamics. For spin rates typical of fin-stabilized projectiles, the trajectory is essentially independent of both bearing resistance and mass ratio.				
14. SUBJECT TERMS smart munitions, projectile aerodynamics, differential roll			15. NUMBER OF PAGES 42	
			16. PRICE CODE	
17. SECURITY CLASSIFICATION OF REPORT UNCLASSIFIED	18. SECURITY CLASSIFICATION OF THIS PAGE UNCLASSIFIED	19. SECURITY CLASSIFICATION OF ABSTRACT UNCLASSIFIED	20. LIMITATION OF ABSTRACT UL	

INTENTIONALLY LEFT BLANK.

USER EVALUATION SHEET/CHANGE OF ADDRESS

This Laboratory undertakes a continuing effort to improve the quality of the reports it publishes. Your comments/answers to the items/questions below will aid us in our efforts.

1. ARL Report Number/Author ARL-CR-455 (Costello) Date of Report July 2000
2. Date Report Received _____
3. Does this report satisfy a need? (Comment on purpose, related project, or other area of interest for which the report will be used.) _____

4. Specifically, how is the report being used? (Information source, design data, procedure, source of ideas, etc.) _____

5. Has the information in this report led to any quantitative savings as far as man-hours or dollars saved, operating costs avoided, or efficiencies achieved, etc? If so, please elaborate. _____

6. General Comments. What do you think should be changed to improve future reports? (Indicate changes to organization, technical content, format, etc.) _____

CURRENT
ADDRESS

Organization

Name

E-mail Name

Street or P.O. Box No.

City, State, Zip Code

7. If indicating a Change of Address or Address Correction, please provide the Current or Correct address above and the Old or Incorrect address below.

OLD
ADDRESS

Organization

Name

Street or P.O. Box No.

City, State, Zip Code

(Remove this sheet, fold as indicated, tape closed, and mail.)
(DO NOT STAPLE)